



Synthesis and Characterization of Molecularly Imprinted Polymers (MIP) based on Methacrylamide (MAM) and EGDMA as a Material to Detect Dibutyl Phthalate (DBP)

St Fauziah^{a,*}, Paulina Taba^a, Muralia Hustim^b, Sulfa Mubarika^a, Janti Kasuaran^a, Husnia Paraditha Husain^a, Ajuk Sapar^c

^a Department of Chemistry, Faculty of Mathematics and Natural Sciences, University of Hasanuddin, Makassar, Indonesia 90245

^b Department of Environmental Engineering, Faculty of Engineering, University of Hasanuddin, Makassar, Indonesia 90245

^c Department of Chemistry, Faculty of Mathematics and Natural Sciences, University of Tanjungpura, Pontianak, Indonesia 78124



Abstract

Molecularly Imprinted Polymer (MIP) has the ability to selectively bind target molecules so that it can be used as an absorbent in the separation process. This study aims to synthesize, characterize, and analyze the optimization of MIP performance. MIP material is synthesized using the precipitation polymerization method which reacts between methacrylamide (MAM) as a monomer, ethylene glycol dimethacrylate (EGDMA) crosslinker, and dibutyl phthalate (DBP) as a template molecule. MIP material is characterized using SEM-EDS, FTIR spectrometer, SAA, and UV-Vis spectrophotometer. The test variables for the adsorption ability of MIP material to DBP compounds are time and concentration. The results of the study showed that the synthesized MIP is a fine and uniform white solid granule. The results of EDS characterization showed a decrease in the atomic mass of C and the percent of C atoms indicating the extraction of DBP from MIP_DBP_MAM-co-EGDMA_(AE). SEM characterization showed a surface morphology of small round grains that tended to be uniform. The functional groups that influenced both polymers obtained from FTIR data were -NH , -CH , -C=C and -C=O . SAA analysis showed that the surface area of MIP_DBP_MAM-co-EGDMA_(AE) was 27.6950 m²/g. The optimum time of MIP_DBP_MAM-co-EGDMA_(AE) adsorption to DBP was 60 minutes according to the pseudo-second-order kinetic model. The adsorption of MIP_DBP_MAM-co-EGDMA_(AE) was in accordance with the Langmuir adsorption isotherm with adsorption capacity values of 2.039 mg/g. The adsorption kinetic model that occurs in MIP follows the pseudo-second-order adsorption kinetic model.

Keywords: polymer; MIP; DBP; methacrylamide

1. Introduction

The use of plastic polymers in everyday life tends to increase because the material is lightweight, airtight, and resistant to temperature changes [1]. In addition, another advantage of these materials is that they are flexible, strong, easy to shape, not easily broken, and electrical insulators [2]. Several plastic material products are all around us, including plastic bags, fiberglass, clothing, polyethylene cups, epoxy glue, Teflon-coated cookware, and others [3]. The main plastic material commonly used is from the polyethylene terephthalate group for making various products such as food and beverage product packaging in industry and viscose for clothing. This type of plastic has strong, tensile, lightweight, transparent, and gas-tight characteristics [4]. Several types of phthalates are widely used as raw materials for manufacturing plastic products, such as dibutyl phthalate (DBP) [5], benzyl butyl phthalate (BBP), dibutyl phthalate and di-isobutylphthalate (DiBP), and bis(2-ethylhexyl)phthalate (DEHP), were found in container water recycled of PET [4][6] and DEHP was decreased in bottle water tests of virgin PET [4].

Besides the advantages, it turns out that the use of plastic has a negative impact because it turns out that the toxic gas produced and the main material used to make plastic itself are dangerous to human health [1]. To ensure the safety and health of consumers, then important to identify the presence of these compounds in beverage and food products. The presence of phthalates such as DBP, DEHP, and others can be a risk to human health. In 2019, using the Gas Chromatography and Liquid Chromatography methods, DBP was found to be 82.8 µg/L and was most detected in bottled drinking water [7]. Phthalates are not easily soluble and pollute the environment because they are not bound to the plastic matrix. Various studies on animals and humans show that phthalates are toxic and interfere with their reproduction [8]. DBP compounds are often detected in the environment, such as soil, air, sediment, food, drinks, and even human body fluids. Therefore, research is needed to

*Corresponding author e-mail: : stfauziah@unhas.ac.id; (St. Fauziah).

Received date 28 December 2024; Revised date 16 April 2025; Accepted date 13 May 2025

DOI: 10.21608/EJCHEM.2025.347820.11056

©2025 National Information and Documentation Center (NIDOC)

spectrophotometrically monitor and detect DBP[9]. Monitoring and detection of DBP can be done by analysis methods based on preconcentration, including solid phase extraction (SPE), extraction of liquid-liquid, and solid phase microextraction (SPME). SPE and SPME methods are considered accurate, superior, and precise methods[10].

The SPE method is one of the sample preparation methods that is widely applied because it has many advantages compared to other extraction methods. The SPE method uses a stationary phase to extract analytes from various different liquid matrices [11]. The SPE is an alternative method to eliminate several disadvantages, such as many organic solvents, high costs, a lengthy operation time, and numerous steps[12]. Therefore, selective materials need to be used for the stationary phase in the SPE method. The selective material is MIP. MIP has optical properties and memory effects on target compounds so that it can be used for separation processes[13]. The MIP is synthesized from functional monomers (MAM) and crosslinking agents (EGDMA) with cavities which are the target molecular (DBP) of the analytes to be extracted. The MIP was characterized to identify its selective sites, sizes, and shapes [14]. EGDMA plays an important role in the formation of MIP[15], as an agent for a three-dimensional polymer network formation[16] and also in the selectivity and binding capacity of MIP [17].

In this study, the synthesis of MIP was carried out using method of the precipitation polymerization. The advantage of MIP synthesis using the precipitation technique is that the material does not undergo crushing and filtering, while synthesis using bulk polymerization involves crushing and filtering. The MIP particles obtained from the precipitation technique are spherical with a more uniform size[13] with the ability to bind target molecules, high selectivity, stability of thermochemical, sensitivity, and reusability[18].

Based on the description, it is necessary to synthesize and characterize MIP-DBP using MAM, EGDMA, and DBP as a template molecule and target molecule. The resulting MIP is used as an adsorbent or stationary phase in the separation process of a compound or mixture. The MIP results obtained were characterized by Fourier Transform Infrared (FTIR), Scanning Electron Microscope (SEM), Energy Dispersive Spectroscopy (EDS), and Surface Area Analyzer (SAA), and its ability to adsorb DBP compounds was analyzed qualitatively and quantitatively analyzed.

2. Experimental

2.1. Material and Equipment

The materials used in this study were dibutyl phthalate (DBP) 99.5% ethylene glycol dimethacrylate (EGDMA) (Sigma Aldrich), (Sigma Aldrich), methacrylamide 99% (MAM) (Sigma Aldrich), 2,2-azobisisobutyronitrile (AIBN) 75% (Sigma Aldrich), acetone, toluene, methanol p.a, acetic acid p.a. (Meck), N₂, Whatman paper no. 42, distilled water and glassware, analytical scales, water baths, shaker, oven, sonicators, bottles, micropipettes, *Ultra Violet Visible* (UV-Vis) spectrophotometer (Shimadzu, UV-2600), *Fourier Transform Infrared* (FTIR) spectrometer (Shimadzu, IR Prestige 21), *Surface Area Analyzer* (SAA) (NOVA, 1200e), *Scanning Electron Microscope* (SEM) and *Energy Dispersive Spectroscopy* (EDS) (JEOL, JSM-6510 LA).

2.2. Procedure of experimental

The procedure of experimental consists of several steps, including synthesis of NIP and MIP, characterization of MIP, optimization of MIP (time and concentration effects), determination of capacity, and kinetics adsorption.

2.3. Synthesis of NIP, MIP-DEHP, and MIP-DBP

DBP liquid was pipetted as much as 0.2651 mL (1 mmol) and mixed with MAM monomer as much as 0.3404 (4 mmol) in a round bottom flask and then left for 5 minutes. After that, the mixture was added with EGDMA crosslinker as much as 3.772 mL (20 mmol) and left for 5 minutes. Furthermore, the mixture was dissolved in 50 mL of toluene, then sonicated for 10 minutes, and then flowed with N₂ for 10 minutes to remove O₂ gas. After that, add 5 mL of AIBN (1 mmol), sonication for 10 minutes, and flowing N₂ for 10 minutes in sequence. The next stage is the polymerization process with heating at a temperature of 60 °C for 24 hours in a water bath [19]. The next stage is polymer washing with methanol, acetone, and aquadest. Furthermore, DBP as a molecule template was extracted for 30 minutes from MIP by sonication using methanol and acetic acid (8: 2 v/v) [20]. The polymer was named MIP-DBP-MAM-co-EGDMA_(BE) and MIP-DBP-MAM-co-EGDMA_(AE) after extraction. The extract was analyzed with a UV-Vis at 263.2 nm to detect the DBP compound. This procedure was repeated until it became zero absorbance. After that, the MIP was washed until the pH was neutral with methanol and distilled water, and then the next stage was the drying process and characterization. NIP or non-imprinted polymers were made without using template molecules in the same way as MIP without the process of extraction. This polymer will be named NIP-MAM-co-EGDMA.

2.4. Characterization of MIP and NIP using SEM-EDS

MIP and NIP materials were prepared by cutting and coating with a conductor layer, after which each was analyzed for surface morphology and atomic distribution using the SEM-EDS instrument.

2.5. Characterization of MIP and NIP using FTIR

MIP and NIP materials were each put into an oven at a temperature of 50 °C. Then the sample was added with KBr at a ratio of 1:10. The mixture was then formed into pellets with a thickness of 3 mm, using a pellet compactor. Furthermore, it was analyzed using FTIR spectrometer[21].

2.6. Characterization of MIP using SAA

The extracted MIP material was weighed and put into a clean sample cell. Then, the gases trapped on the surface of the MIP material were removed. Furthermore, it was analyzed using the SAA instrument [22]. NIP and MIP_DBP polymers were characterized, qualitatively, and quantitatively analyzed using SEM-EDS, FTIR, and SAA.

2.7. Adsorption Ability Test of NIP, MIP_DEHP and MIP_DBP

An amount of 30 mg of each MIP and NIP were put into vials that had been prepared, then 5 mL of 10 mg/L DBP solution was added to the vials. The mixture was stirred for 60 minutes and then filtered. Furthermore, the DBP concentration in the filtrate was analyzed using a UV-Vis at the maximum wavelength. The total of DBP compound adsorbed in each gram of MIP and NIP was calculated using Equation (1) [23]:

$$q = \frac{(C_0 - C_e) V}{m} \quad (1)$$

Description:

q = Capacity of adsorption (mg/g).

v = Volume of solution (L)

C₀ = Concentration of initial solution (mg/L)

C_e = Concentration of solution after adsorption process (mg/L)

m = MIP mass used (g)

A total of 30 mg of MIP and 5 mL DBP standard solution were put into 5 vials, then stirred with time variations of 10, 30, 60, 120, and 150 minutes. After the adsorption process, the solution was analyzed using a UV-Vis at the maximum wavelength. The study of adsorption kinetics was calculated using pseudo-first and second-order kinetic models [24].

2.8. Concentration Effect on DBP Adsorption by MIP

A total of 5 mL of DBP solution with concentration variations, namely 9, 12, 15, 18, and 24 mg/L, were mixed with 30 mg of MIP, and then stirred with a shaker for 60 minutes. Furthermore, the solution was filtered and determined with a UV spectrophotometer at the maximum wavelength.

2.9. Adsorption kinetics determination of MIP

Adsorption kinetics can be determined from the analysis data of the effect of time using pseudo-first (equation 2) and second-order (equation 3) [25], [24]:

$$\frac{dq_t}{dt} = k_1 (q_e - q_t) \quad (2)$$

Description:

q_t = Total of adsorbate adsorbed (mg/g)

q_e = Adsorption capacity equilibrium (mg/g)

k₁ = Pseudo-first order constant (/minute)

t = Time of contact (minute)

$$\frac{dq_t}{dt} = k_2 (q_e - q_t)^2 \quad (3)$$

Description:

k₂ = adsorption rate constant at pseudo-second order (/minute)

2.10. Adsorption capacity determination of MIP

The adsorption capacity was analyzed of the concentration effect data using the Freundlich adsorption isotherm equation and the Langmuir isotherm [20]. The Equation of Langmuir adsorption isotherm is calculated in Equation (4), and the Freundlich adsorption isotherm equation is stated in Equation (5) [26]:

$$\frac{C_e}{q_e} = \frac{1}{K_L q_m} + \frac{C_e}{q_m} \quad (4)$$

$$\log q_e = \frac{1}{n} \log C_e + \log K_F \quad (5)$$

Description:

C_e = Concentration at equilibrium in solution (mg/L)

q_m = Maximum of adsorption capacity (mg/g)

q_e = Amount of adsorbed substance at equilibrium (mg/g)

K_L = Constant of affinity (L/mg)

K_F = Adsorption capacity (mg/g)

$1/n$ = Heterogeneity factor

3. Results and Discussion

MIP material has been produced in the white solid form. The synthesized polymer was extracted to remove the DBP template molecule using methanol and acetate solvents. The DBP compound that has been extracted from the polymer was determined using a UV-Vis at a wavelength of 263.2 nm, and the resulting data is in Table 1. Table 1 shows that the concentration of extracted DBP decreases. This is indicated by a decrease in the absorbance or absorption value of each extract.

Table 1. Qualitative test of DBP compounds that have been extracted with a mixture of methanol: acetic acid (8:2) solvents with a UV spectrophotometer.

DBP Extracts	Absorbance (nm)
Ex.-1	1.407
Ex.-2	1.003
Ex.-3	0.551
Ex.-4	0.350
Ex.-5	0.264
Ex.-6	0.195
Ex.-7	0.178
Ex.-8	0.161
Ex.-9	0.060
Ex.-10	0.026

This indicates that the dibutylphthalate (DBP) compound has been extracted from MIP. According to Jupri et al. (2022[27], there are three stages that occur in the synthesis process of MIP_DBP_MAM-co-EDGMA, namely pre-polymerization stage, polymerization, and extraction of the dibutyl phthalate (DBP) template molecule from the MIP matrix. The depiction of the reaction at each stage of the synthesis is shown in Figure 1.

In the pre-polymerization stage (a), DBP template molecules and MAM monomers first interact non-covalently in the toluene solvent to form hydrogen bonds. In polymerization stage (b), EDGMA crosslinker and MAM monomer form a polymer matrix initiated by AIBN. The polymerization process covers the initiation, propagation, and termination.

The next stage is the extraction stage (c), the release of DBP molecules contained in the polymer to obtain a template according to the DBP compound as the of DBP molecules contained in the polymer to obtain a template according to the DBP compound as the hydrogen bonds with functional groups contained in the DBP template. The MIP synthesized can be characterized using FTIR, SEM, EDS, and SAA instruments. Functional groups in the DBP compound can interact non-covalently to form hydrogen bonds.

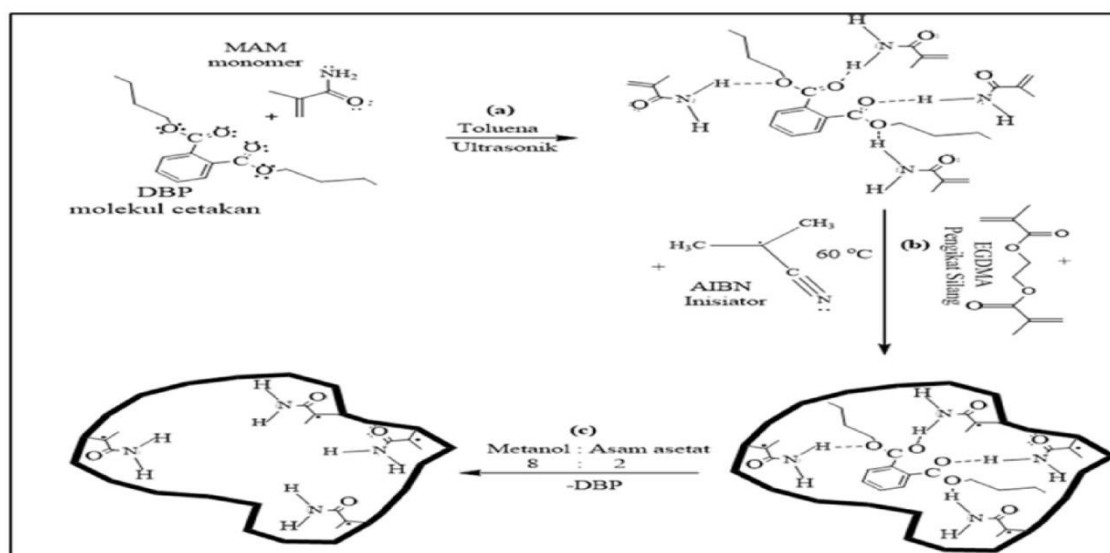


Figure 1. Reaction scheme of MIP_DBP_MAM-co-EGDMA synthesis, (a) pre-polymerization stage, (b) polymerization stage, and (c) template molecule extraction stage

3.1 Characterization of MIP and NIP

3.1.1 Characterization of MIP and NIP using EDS

EDS analysis was conducted to determine the main atomic composition of the polymers NIP_MAM-co-EGDMA, MIP_DBP_MAM-co-EGDMA_(BE), MIP_DBP_MAM-co-EGDMA_(AE), which are C (Carbon), O (Oxygen), N (Nitrogen), and H (Hydrogen). The EDS analysis data are in Table 2, which only shows the mass percentage of C, O, and N. The atomic mass of H is not listed because it is very small and difficult to detect. The mass percentage and atomic percentage of C are used to determine how much the percentage of carbon atoms or mass decreases due to DBP molecules being released from the polymer to indicate the synthesis success of MIP_DBP_MAM-co-EGDMA_(AE). EDS value of NIP_MAM-co-EGDMA, MIP_DBP_MAM-co-EGDMA_(BE), MIP_DBP_MAM-co-EGDMA_(AE) displayed in Table 2.

Table 2. EDS value for NIP_MAM-co-EGDMA, MIP_DBP_MAM-co-EGDMA_(BE), MIP_DBP_MAM-co-EGDMA_(AE)

Elements	% Mass			% Atom		
	NIP	MIP _(BE)	MIP _(AE)	NIP	MIP _(BE)	MIP _(AE)
C	42.15	42.23	42.18	48.81	48.92	48.88
O	50.60	50.91	51.30	43.99	44.27	44.64
N	7.24	6.85	6.52	7.19	6.81	6.48

The percent mass and atomic of C for MIP_DBP_MAM-co-EGDMA_(BE) shown in Table 2 are higher than MIP_DBP_MAM-co-EGDMA_(AE), while the mass percent O and atomic percent O of MIP_DBP_MAM-co-EGDMA_(BE) are lower than MIP_DBP_MAM-co-EGDMA_(AE) cause the number of C atoms greater than O atom in DBP, so that when DBP stay in the polymer, mass % of C and the atom % of C increase, while when DBP is released from the MIP, the mass % of O and the atom % of O will increase while the atom % of C decreases.

The decrease in the mass percentage of C and the percentage of C atoms is 0.05% and 0.04% respectively, indicating that the DBP compound has been released from MIP. The small mass percentage and atom of C lost are due to the small amount of DBP in the polymer when compared to the mass and atom percentage of C in MIP formed from MAM monomers and EGDMA crosslinkers.

3.1.2 MIP and NIP Characterization using SEM

The surface morphology of the synthesis results of NIP_MAM-co-EGDMA, MIP_DBP_MAM-co-EGDMA_(BE), MIP_DBP_MAM-co-EGDMA_(AE) using SEM in Figure 2.

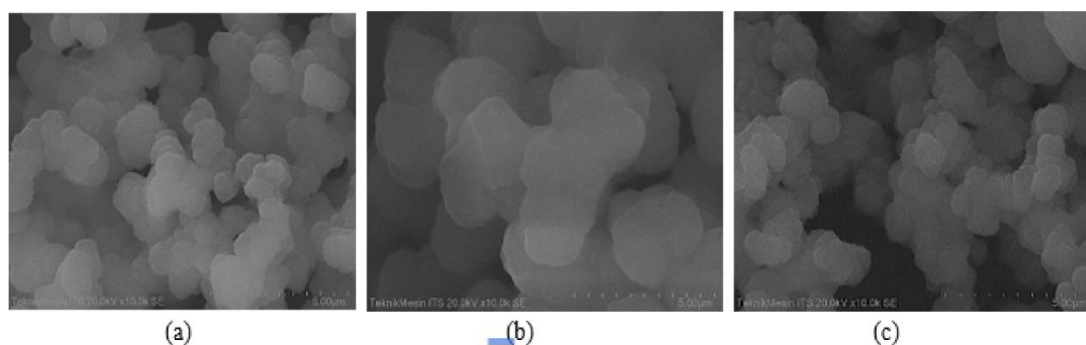


Figure 2. Surface morphology with 10,000x magnification using SEM for (a) NIP_MAM-co-EGDMA, (b) MIP_DPB_MAM-co-EGDMA(BE), (c) MIP_DPB_MAM-co-EGDMA(AE)

The MIP surface morphology is a small granule with densities and different sizes. The surface morphology of NIP_MAM-co-EGDMA (a) consists of small granules with a non-uniform shape and is denser. Meanwhile, the surface morphology of MIP_DPB_MAM-co-EGDMA_(BE) (b) and MIP_DPB_MAM-co-EGDMA_(AE) (c) is composed of round grains with sizes that tend more uniform. The surface morphology of MIP_DPB_MAM-co-EGDMA_(BE) looks more unified compared to MIP_DPB_MAM-co-EGDMA_(AE).

3.1.3 Characterization of MIP and NIP using FTIR

Characterization using FTIR aims to determine bonding formation for the synthesis process. The chemical bonds or functional groups in MIP and NIP change in absorption intensity and wave number shift. The FTIR spectrum is presented in Figure 3. Functional groups that affect the formation of NIP_MAM-co-EGDMA, MIP_DPB_MAM-co-EGDMA_(BE), and MIP_DPB_MAM-co-EGDMA_(AE) can be seen in Table 3.

Table 3. Wave number data from FTIR analysis results for MAM monomers, NIP_MAM-co-EGDMA, MIP-DBP-MAM-co-EGDMA_(BE), and MIP-DBP-MAM-co-EGDMA_(AE).

Functional groups	Wave number (cm ⁻¹)			
	MAM monomer	NIP_MAM-co-EGDMA	MP_DBP_MAM-co-EGDMA _(BE)	MP_DBP_MAM-co-EGDMA _(AE)
-NH stretching	3385.07	3570.24	3568.31	3566.38
-C=O stretching	1668.43	1730.15	1730.15	1730.15
-C=C stretching	1602.85	1670.35	1662.64	1662.64

The absorption peaks of the functional groups owned by NIP and MIP, namely -NH, -C=O, -C=C experienced a shift in wave number after being involved in interaction with MAM monomers and EGDMA crosslinkers during the polymer formation process. The absorption peak of the -NH of NIP_MAM-co-EGDMA, MIP_DPB_MAM-co-EGDMA_(BE), and MIP_DPB_MAM-co-EGDMA_(AE) changes compared to the MAM due to the reduced basicity of the monomer after formation of the polymer. Table 3 shows that the -NH functional group in the MIP_DPB_MAM-co-EGDMA_(BE) and MIP_DPB_MAM-co-EGDMA_(AE) undergoes a small wave number shift.

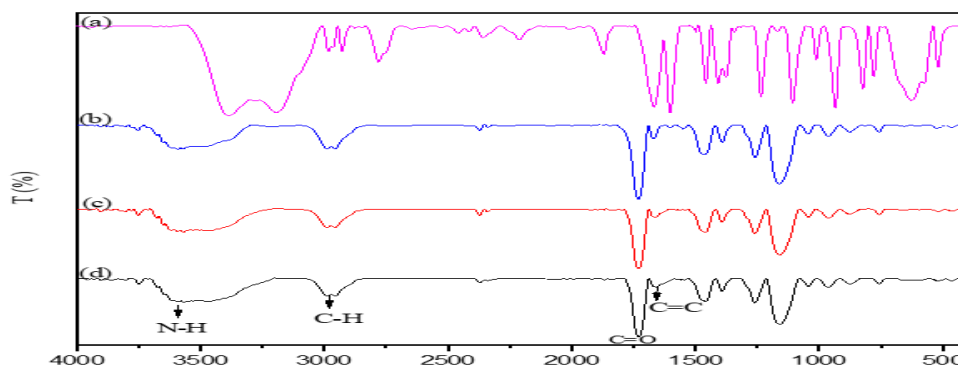


Figure 3. FTIR spectrum (a) MAM monomer, (b) NIP_MAM-co-EGDMA, (c) MIP_DPB_MAM-co-EGDMA_(BE), (d) MIP_DPB_MAM-co-EGDMA_(AE)

The absorption intensity of MIP_DBP_MAM-co-EGDMA_(AE) is stronger than the absorption intensity of MIP_DBP_MAM-co-EGDMA_(BE); this is because the hydrogen bond has been broken between the -NH functional group in the polymer and the DBP template molecule.

The -CH bonds in the three polymer materials, namely NIP_MAM-co-EGDMA, MIP_DBP_MAM-co-EGDMA_(BE), and MIP_DBP_MAM-co-EGDMA_(AE) experience a fairly large wave number shift compared to the MAM functional monomer. The addition reaction that occurs after the polymer is formed in the MAM monomer causes a change in -CH sp² to -CH sp³, so that the absorption of the -CH bonds in the three MIP materials is higher compared to the MAM monomer. The -C=C bond in the NIP_MAM-co-EGDMA, MIP_DBP_MAM-co-EGDMA_(BE), and MIP_DBP_MAM-co-EGDMA_(AE) materials has a wave number value that is much larger than the -C=C vibration in the MAM monomer. This is because the double bond has been broken into a single bond due to the polymerization process by the initiator in the monomer and crosslinker that forms the polymer matrix. The -C=O bond in the three polymer materials NIP_MAM-co-EGDMA, MIP_DBP_MAM-co-EGDMA_(BE), and MIP_DBP_MAM-co-EGDMA_(AE) did not experience a wave number shift. This is because the -NH group in the MAM monomer with the -C=O group in DBP interacts to form a hydrogen bond so that there is no shift in the -C=O group for the NIP_MAM-co-EGDMA, MIP_DBP_MAM-co-EGDMA_(BE), and MIP_DBP_MAM-co-EGDMA_(AE) materials when compared to the MAM monomer. Based on the FTIR data, the functional groups contained in the formation of NIP_MAM-co-EGDMA and MIP_DBP_MAM-co-EGDMA are -NH, -C=O, and -C=C.

3.1.4 MIP Characterization Using SAA

Surface area analysis of MIP_DBP_MAM-co-EGDMA_(AE) was determined using SAA with the Brunauer-Emmett-Teller (BET) to identify adsorbent and pores area. Measurements were made based on isotherm adsorption data at 77.3 K. The amount of N₂ adsorbed was the basis for calculating the surface area. The measurement results showed MIP_DBP_MAM-co-EGDMA_(AE) surface area was 27.696 m²/g. SAA analysis using the Barret-Joyner-Hallenda (BJH) method was carried out to ensure the specific surface area, volume, and pore MIP diameter. However, in this study, the results obtained for pore volume and pore diameter were not detected. This can be caused by several factors, including the polymerization technique, which causes the imprinted molecules not to be completely released from the MIP [28]. Too strong a bond can also cause the target molecule to be unable to escape so that the MIP has a closed cavity and cannot be detected. The pore size is too small which causes the BJH method for characterizing this MIP to be ineffective.

3.1.5 DBP Adsorption by MIP and NIP

The obtained MIP_DBP_MAM-co-EGDMA_(AE) and NIP_MAM-co-EGDMA were analyzed for their adsorption capacity. The total of DBP adsorbed can be seen in Figure 4.

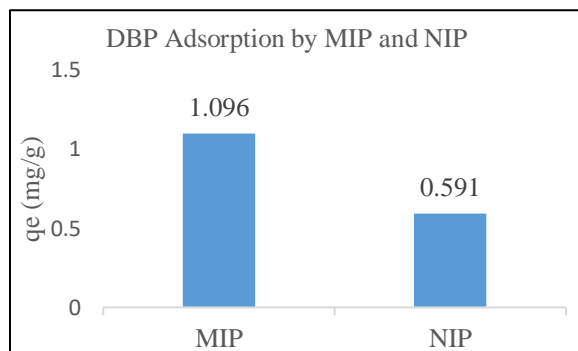


Figure 4. DBP Adsorption by MIP and NIP

Figure 4 describes that the adsorption capacity of MIP material is better than NIP material with a Δq_e value of 0.506 mg/g as the amount difference of DBP adsorbed. Both materials need to be optimized to determine the maximum adsorption capacity. Optimization was conducted with various adsorption parameters, including contact time and concentration effect.

3.1.6 Effect of Time on DBP Adsorption by MIP

The effect of time on the adsorption capacity of DBP compounds by MIP can be seen in Figure 5. The adsorbed DBP increases with increasing contact time to reach maximum adsorption. This is because contact time has a great influence on determining the adsorption ability of MIP. When maximum adsorption is achieved, the saturation point of MIP is estimated to have been reached in adsorbing DBP so that when time is increased, the adsorption capacity will decrease. The optimum time for MIP_DBP_MAM-co-EGDMA_(AE) to adsorb DBP is 60 minutes with the amount of adsorbed compound as much as 1.19 mg/g. The research data based on time effect were analyzed using pseudo-first and second-order equations.

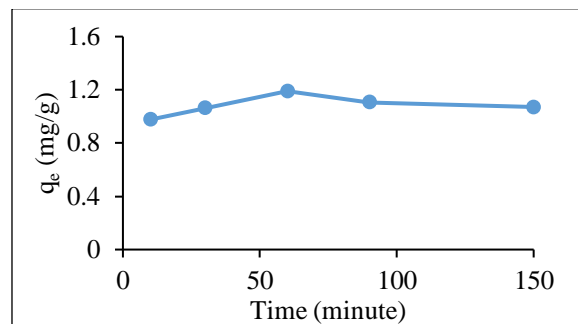


Figure 5. Time effect of DBP adsorbed by MIP-DBP-MAM-co-EGDMA_(AE)

3.1.7 Effect of Concentration on DBP Adsorption by MIP

The effect of concentration on the DBP adsorption by MIP is displayed in Figure 6. The higher concentration of DBP was adsorbed by MIP-DBP-MAM-co-EGDMA_(AE). The adsorption capacity of MIP-DBP-MAM-co-EGDMA_(AE) at the optimum time will increase when the concentration is increased. When the adsorption has reached the maximum and equilibrium limit, the adsorption capacity of MIP-DBP-MAM-co-EGDMA_(AE) tends to remain the same even though the concentration is increased. The amount of DBP adsorbed still increases in the concentration range worked on, so the adsorption capacity is added using the adsorption isotherm model.

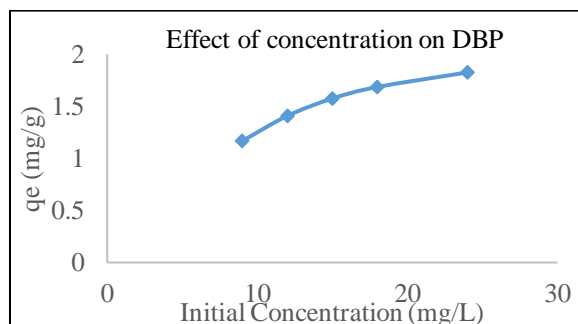
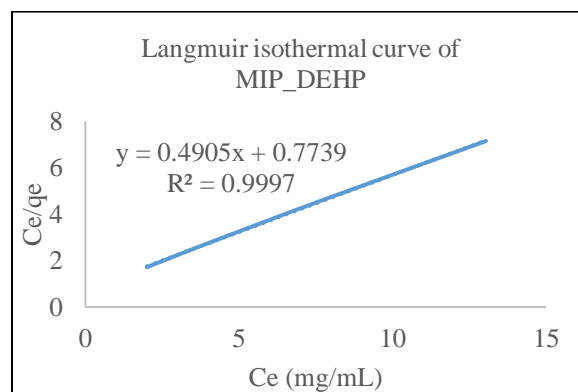


Figure 6. Effect of concentration on DBP adsorbed by MIP-DBP-MAM-co-EGDMA_(AE).

The adsorption capacity of MIP-DBP-MAM-co-EGDMA_(AE) can be determined by the Freundlich and Langmuir adsorption isotherm models. The appropriate adsorption isotherm model is obtained from the linearity curve. The linearity of Langmuir isotherm curve is the relationship between C_e and C_e/q_e obtained from equation (2). While the linearity of the Freundlich isotherm curve is the relationship between $\log q_e$ and $\log C_e$ obtained from equation (3). Adsorption isotherm curves of Langmuir and Freundlich are displayed in Figure 7.



(a)

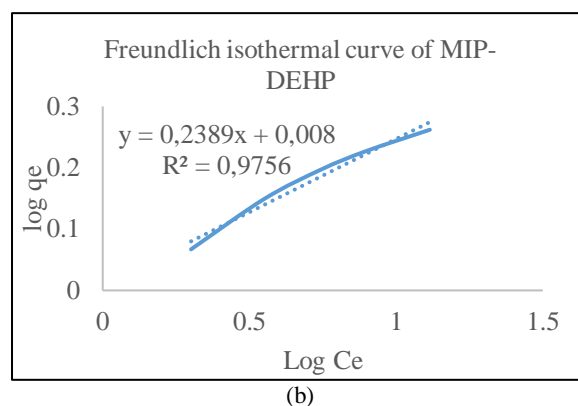


Figure 7. Langmuir (a) and Freundlich (b) adsorption isotherm curves of DBP adsorption by MIP_DBP_MAM-co-EGDMA_(AE)

Figure 7 shows that the correlation coefficient value from the Langmuir isotherm adsorption curve (a) for MIP_DBP_MAM-co-EGDMA_(AE) is 0.9997, while the correlation coefficient value obtained from the Freundlich isotherm adsorption curve (b) for MIP_DBP_MAM-co-EGDMA_(AE) is 0.9751. The adsorption parameter data of each adsorption isotherm mode are shown in Table 4.

Table 4. DBP adsorption parameter data by MIP_DBP_MAM-co-EGDMA_(AE) obtained from the Langmuir adsorption isotherm curve and the Freundlich adsorption

Type of MIP	Langmuir adsorption isotherm			Freundlich adsorption isotherm		
	K_L (L/mg)	q_m (mg/g)	R^2	K_F (mg/g)	N	R^2
MIP_DBP_MAM-co-EGDMA _(AE)	0.633	2.039	0.999	1.018	4.191	0.975

The R^2 value for MIP_DBP_MAM-co-EGDMA_(AE) for the Freundlich isotherm adsorption model is greater than the R^2 value for the Langmuir isotherm adsorption model. Thus, the Langmuir adsorption isotherm model is used to determine the adsorption capacity of DBP compounds by MIP_DBP_MAM-co-EGDMA_(AE). The Langmuir adsorption isotherm indicates that adsorption occurs on a homogeneous or monolayer adsorbent surface. After the adsorbate occupies one area on the adsorbent, no further adsorption occurs in that area. Table 4 shows the Q_m value of 2.039 mg/g, which is the maximum adsorption capacity of MIP_DBP_MAM-co-EGDMA_(AE).

The Langmuir constant (K_L) of MIP_DBP_MAM-co-EGDMA_(AE) is 0.663 L/mg. The R_L value obtained in the Langmuir isotherm was obtained on average at 0.1006 mg/L. The R_L value of $0 < R_L < 1$ indicates that the adsorption is highly selective which is calculated using Equation (6).

$$R_L = \frac{1}{1 + K_L C_0} \quad (6)$$

Description:

R_L = Concentration at equilibrium in solution (mg/L)

K_L = Affinity constant (L/mg)

C_0 = Initial concentration (mg/L)

If $R_L > 1$ is obtained, it means that the adsorption is not selective and if $R_L = 1$ means that the adsorption is selective and linear [29].

4. Conclusions

Based on the research that has been done, it can be concluded that MIP_DBP_MAM-co-EGDMA material can be synthesized by the precipitation polymerization method, which produces a polymer with a fine white granular form. The characterization result with EDS shows a decrease in the mass percentage of C and atomic percentage of N, which indicates the formation of MIP_DBP_MAM-co-EGDMA_(AE). The surface morphology from SEM characterization results of MIP_DBP_MAM-co-EGDMA material is composed of small round granules that tend to be uniform. The vibrations that affect the polymer formation are $-NH$, $-CH$, $-C=O$ and $-C=C$. The surface area of MIP_DBP_MAM-co-EGDMA_(AE) is 27.6950 m²/g. The optimum adsorption time of MIP_DBP_MAM-co-EGDMA_(AE) to DBP is 60 minutes according to the pseudo second order kinetic model.

5. Conflicts of interest: There are no conflicts to declare

6. Acknowledgments

Thank you for the financial support for Regular Fundamental Research of State University Operational Assistance Program (BOPTN), Directorate of Research, Technology, and Community Service (DRTPM), Indonesia 2024 with contact number 0459/E5/PG.02.00/2024 and Contract agreement number 02035/UN4.22.2/PT.01.03/2024.

7. References

- [1] Jiamin Lu., Polymer Materials in Daily Life: Classification, Applications, and Future Prospects. *E3S Web of Conferences*, 01034. doi: 10.1051/406 e3sconf/202340601034 (2023)
- [2] Hendrawati, Agus Rimus Liandi, Mar'atus Solehah, Mohammad Herga Setyono, Isalmi Aziz, Yusraini Dian Inayati Siregar Pyrolysis of PP and HDPE from plastic packaging waste into liquid hydrocarbons using natural zeolite Lampung as a catalyst. *Case Studies in Chemical and Environmental Engineering*. **7**, 100290. doi: 10.1016/j.cscee.2022.100290 (2023)
- [3] Hasan Namazi, Polymers in our daily life, *BioImpacts*, **7**(2), 73–74. doi: 10.15171/bi.2017.09 (2017)
- [4] Vaishali Dhaka, Simranjeet Singh, Amith G. Anil, T. S. Sunil Kumar Naik, Shashank Garg, Jastin Samuel, Manoj Kumar, Praveen C. Ramamurthy, Joginder Singh, Occurrence, toxicity, and remediation of polyethylene terephthalate plastics. A review. *Environmental Chemistry Letters* **20**:1777–1800. doi:10.1007/s10311-021-01384-8 (2022)
- [5] Junliang Shen, Wenming Yang, Wenjie Zhu, Junhao Che, Hua Ding, Fei Song, Wenwen Zhang, Pengfei Jiang, Wanzhen Xu, Weihong Huang, Preparation and characterisation of photoresponsive molecularly imprinting polymer nanoparticles with hollow structure for extraction and enrichment of dibutyl phthalate, *Reactive and Functional Polymers*, Volume 186, 105536 (2023). doi: 10.1016/j.reactfunctpolym.2023.105536
- [6] Keresztes S, Tatár E, Czégény Z et al Study on the leaching of phthalates from polyethylene terephthalate bottles into mineral water. *Sci Total Environ*. 458–460:451–458. Doi: 10. 1016/j.scitotenv.2013. 04. 056 (2013)
- [7] Rouse da Silva Costa, Tatiana Sainara Maia Fernandes, Edmilson de Sousa Almeida, Juliene Tomé Oliveira, Jhonyson Arruda Carvalho Guedes, Guilherme Julião Zocolo, Francisco Wagner de Sousa, Ronaldo Ferreira do Nascimento, Potential risk of BPA and phthalates in commercial water bottles: a minireview. *Water Health*. **19**(3):411-435. doi: 10.2166/wh.2021.202 (2021)
- [8] Sapna Sedha, Hoomin Lee, Siddhartha Singh, Sunil Kumar, Subodh Jain, Ajaz Ahmad, Yousef A. Bin Jordan, Sonam Sonwal, Shruti Shukla, Jesus Simal-Gandara, Jianbo Xiao, Yun Suk Huh, Young-Kyu Ha, Vivek K. Bajpai, Review: Reproductive toxic potential of phthalate compounds – State of art review. *Pharmacological Research*. **167**: 105536 (2021)
- [9] Zhou Q., Guo M., Wu S., Fornara D., Sarkar B., Sun L. and Wang, H., Electrochemical Sensor Based on Corncob Biochar Layer Supported Chitosan-MIPs for Determination of Dibutyl Phthalate (DBP), *Journal of Electroanalytical Chemistry*, **897** (2021).
- [10] Bolat G., Yaman Y.T., and Abaci S., Molecularly Imprinted Electrochemical Impedance Sensor for Sensitive Dibutyl Phthalate (DBP) determination, *Sensor and Actuators B: Chemical*, 299: 1-9 (2019).
- [11] Berthod L., Roberts G. and Mills G.A., A Solid-Phase Extraction Approach for the Identification of Pharmaceutical-Sludge Adsorption Mechanisms, *Journal of Pharmaceutical Analysis*, **4**(2): 117-124 (2014).
- [12] Mohamed E. I. Badawy, Mahmoud A. M. El-Nouby, Paul K. Kimani, Lee W. Lim, Entsar I. Rabea, A review of the modern principles and applications of solid-phase extraction techniques in chromatographic analysis, *Analytical Sciences* **38**:1457–1487. doi:10.1007/s44211-022-00190-8 (2022)
- [13] Kamaruzaman S., Nasir N.M., Mohd Faudzi S.M., Yahaya N., Mohamad Hanapi N.S., Wan Ibrahim W.N., Solid-Phase Extraction of Active Compounds from Natural Products by Molecularly Imprinted Polymers: Synthesis and Extraction Parameters. *Polymers*. **13**, 3780. doi:10.3390/polym13213780 (2021)
- [14] Silva C.F., Menezes L.F., Pareira A.C., and Nascimento C.S., Molecularly, imprinted Polymer (MIP) for Thiamethoxam: A Theoretical and Experimental Study, *Journal of Molecular Structure*, 1231(2021): 1-7 (2021).
- [15] Enas Amoure Hadi; Yehya Kamal Al-Bayati, Preparation and characterized study of new molecularly imprinted polymers for determination Cocaine by GC-Mass based on different Functional Monomers, *Egyptian Journal of Chemistry*, Volume 65, Issue 1, January 2022, Pages 107-116. doi: 10.21608/ejchem.2021.78126.3817
- [16] Fadhel Ibrahim Aljabari, Yehya Kamal Al-Bayati, Estimation of Trimethoprim by using a New Selective Electrodes dependent on Molecularly Imprinted Polymers, *Egypt. J. Chem.* Vol. 64, No. 10 pp. 6089 - 6096 (2021). doi: 10.21608/EJCHEM.2021.72564.3617

- [17] Chen L., Wang X., Lu W., Wu X., and Li J., Molecular Imprinting: Prespectives and Applications, *Chemical Society Reviews*, **45**: 2137-2211 (2016)
- [18] Despina A. Gkika, Athanasia K. Tolkou, Dimitra A. Lambropoulou, Dimitrios N. Bikiaris, Petros Kokkinos, Ioannis K. Kalavrouziotis and George Z. Kyzas, Application of molecularly imprinted polymers (MIPs) as environmental separation tools. *RSC Appl. Polym.*, **2**, 127-148. doi: 10.1039/D3LP00203A (2024)
- [19] Tabarestani M.S., Rahnama K., Jahanshahi M., Nasrollanejad S., and Fatemi M.H., Synthesis of a Nanoporous Molecularly Imprinted Polymers for Dibutyl Phthalate Extracted from *Trichoderma harzianum*, *Journal Nanostructure*, **6**(3); 245-249C (2016)
- [20] Yang Z., Chen F., Tang Y., and Li S., Selective Adsorption of Di-(2-ethylhexyl) Phthalate by Surface Imprinted Polymers with Modified Silica Gelas Functional Support, *Journal of Chemistry Society Pak.*, **37**(5); 939-949 (2015)
- [21] St Fauziah, Nunuk Hariani Soekanto, Prastawa Budi, Herlina Rasyid, Nur Haedar, Muralia Hustim, Marlina Marlina, Magfirah Sulaiman, Ajuk Sapar. Synthesis of molecularly printed methyl methacrylate--based polymers for the detection of di(2-ethylhexyl) phthalate and dibutyl phthalate. *Polimery*. **68**, nr 7-8 (2023)
- [22] Dewi A.P., Manurung P., and Safriadi, Pengaruh Waktu Penambah Doping Sulfur terhadap Luas Permukaan dan Struktur Kristal Nanotitania Menggunakan Metode Sol Gel, *Journal of Energy, Material, and Instrumentation Technology*, **2**(2): 66-71 (2021)
- [23] Zhou T., Tao Y., and Jin H., Fabrication of a Selective and Sensitive Sensor Based on Molecularly Imprinted Polymer/Acetylene Black for the Determination of Azithromycin in Pharmaceuticals and Biological Samples, *Plos One*, 1-15 (2016)
- [24] Lima E.C., Adebayo M.A., and Machado F.M., Kinetic and Equilibrium Models of Adsorption, *Carbon Nanostructures*, **1**(3): 33-69 (2015).
- [25] Dai C., Zhang J., Zhang Y., Zhou X., and Liu S., Application of Molecularly Imprinted Polymers to Selective Removal of Clofibric Acid from Water, *Plos One*, **8**(10); 1-8 (2013).
- [26] Shams Kalam, Sidqi A. Abu-Khamsin, Muhammad Shahzad Kamal, and Shirish Patil. Surfactant Adsorption Isotherms: A Review. *ACS Omega*. **6**, 32342-32348. doi:10.1021/acsomega.1c04661 (2021)
- [27] Jupri R., Fauziah S., and Taba P., Synthesis and Characterization of Molecularly Imprinted Polymers using Methyl Methacrylate and Ethylene Glycol Dimethacrylate as Adsorbent Di-(2-Ethylhexyl) Phthalate. *Indonesian Journal of Pure and Applied Chemistry*, **5**(3): 105-120 (2022). Doi: 10.26418/indonesian.v5i3.59132
- [28] Mustafa Y.L., Keirouz A., and Leese H.S., Molecularly Imprinted Polymers in Diagnostic: Accessing Analytes in Biofluids, *Journl of Materials Chemistry B*, **10**, 7418-7449 (2022)
- [29] Perdana A., Zakrasi A., Hamdani D., Natalisanto A.I., and Munir R., Karakterisasi Adsorben Ampas The dalam Menyerap Ion Logam Timblu menggunakan Model Isoterm Langmuir, *Jurnal Ilmu dan Inovasi Fisika*, **7**(1): 90-97 (2023).